Optical Engineering

OpticalEngineering.SPIEDigitalLibrary.org

Intensity-based method for selection of valid interferometric data in temporal phase shifting interferometry

Jaime Sánchez-Paredes
Gilberto Silva-Ortigoza
Jorge Castro-Ramos

SPIE.

Intensity-based method for selection of valid interferometric data in temporal phase shifting interferometry

Jaime Sánchez-Paredes,[a] Gilberto Silva-Ortigoza,[b,c] and Jorge Castro-Ramos[a,*]
[a]Instituto Nacional de Astrofísica Óptica y Electrónica, Apartado Postal 51 y 216, C.P. 72000, Tonantzintla, Puebla, México
[b]Facultad de Ciencias Físico Matemáticas de la Benemérita Universidad Autónoma de Puebla, Apartado Postal 1152, Puebla 72001, México
[c]Centro de Investigación y de Estudios Avanzados del I.P.N., Departamento de Física, Apartado Postal 14-740, 07000 México, D. F., México

Abstract. In this paper, we propose a method to detect the valid phase pixels of fringe patterns obtained with phase shifting interferometry. From a set of simulated interferogram images, we obtain a set of equations to discriminate between valid and invalid wavefront phase pixels, which allow us to compute the wavefront aberration. This method is useful for testing any converging optical system in a quantitative way with either a small or large focal ratio, with either polished or rough surfaces and with wavefront or lateral shear interferograms. © *2015 Society of Photo-Optical Instrumentation Engineers (SPIE)* [DOI: 10.1117/1.OE.54.2.024106]

Keywords: instrumentation; metrology; phase shift; phase unwrapping; valid phase data.

Paper 141294 received Aug. 15, 2014; accepted for publication Jan. 19, 2015; published online Feb. 18, 2015.

1 Introduction

Optical interference is due to the interaction of two or more light waves, giving a resultant irradiance that deviates from the sum of the component irradiances. The device that allows us to see it is the optical interferometer, which has made possible a great variety of precision measurements. In this paper, we propose a method to detect the valid phase pixels of the fringe patterns obtained with phase shifting interferometry (PSI). This method can be applied to a set of interferograms acquired from either wavefront or lateral shear interferometers. We use a lateral shear interferometer, the Ronchi tester, to show the utility of our results and one wavefront interferometer, the Twyman–Green, to validate our derived background equations.[1,2] Furthermore, instead of the recorded intensity modulation equation, we use the geometrical moments described by Mukundan and Ramakrishnan[3] to obtain a mask of the valid phase pixels. Finally, by using the Ghiglia's method,[4] we unwrap the wavefront phase difference. More specifically, first from a set of simulated interferogram images we obtain a set of equations that we call the background equations to discriminate between valid and invalid wavefront phase pixels. Second, with a charge-coupled device (CCD) camera, we digitized a set of real interferograms and by using our background equations we obtain their associated valid phase pixels. Then, we develop software on Visual C++ 2012 to unwrap and compute the wavefront aberration function of any converging optical system. Finally, we prove the validity of our equations by comparing our results to those obtained by using Durango interferometry software.[5]

2 Interferometry

It is well known that one of the applications of the interferometry technique is to test optical systems which usually use electromagnetic waves. That is, one sends the beam to the interferometer and it splits into two beams. One of them goes to some components of the interferometer and it does not experience any changes. For this reason it is known as the reference beam and is described by $w_r(x,y,t) = a_r(x,y)e^{i[\phi_r(x,y)-\delta(t)]}$, where $a_r(x,y)$ is the amplitude, $\delta(t)$ is the temporal phase, and $\phi_r(x,y)$ is the spatial phase of the beam. The other part of the beam goes through the optical system under test and for this reason, it is known as the test beam. It is assumed that it is described by $w_t(x,y,t) = a_t(x,y)e^{i\phi_t(x,y)}$, where $a_t(x,y)$ is the amplitude and $\phi_t(x,y)$ is the spatial phase of the beam. Therefore, at the interference region, the resulting intensity pattern is given by[2]

$$I(x,y,t) = I(x,y)' + I(x,y)''\mathrm{Cos}[\phi(x,y) + \delta(t)], \tag{1}$$

where $I(x,y)' = a_r^2(x,y) + a_t^2(x,y)$ is the average intensity, $I(x,y)'' = 2a_r(x,y)a_t(x,y)$ is the fringe or intensity modulation, and $\phi(x,y) = \phi_t(x,y) - \phi_r(x,y)$ is the wavefront phase difference. Remember that the aim of the present work is to obtain a set of equations to get the valid phase pixels and use those to recover the wavefront of the emerging beam that has interacted with the optical system under test. Equation (1) is the fundamental equation for PSI.[2] It is important to note that one way to determine the valid phase pixels of a set of interferograms is to use the data modulation $\gamma(x,y)$ across the interferogram, also called the recorded intensity modulation

$$\gamma(x,y) = \frac{I(x,y)''}{I(x,y)'}, \tag{2}$$

2.1 *Phase Shifting Interferometry and Hariharan Algorithm*

The PSI method consists of changing the temporal phase of the incident beam to recover the associate emerging

*Address all correspondence to: Jorge Castro-Ramos, E-mail: jcastro@inaoep.mx

wavefront from the interferograms obtained in any optical test. It is important to note that the PSI method requires at least three changes in the temporal phase. The Hariharan algorithm[6] is one of those methods which uses five changes in the temporal phase. That is, it is a five-step algorithm and thus requires that five separate interferograms of the system under test must be recorded and digitized. In this algorithm, the function $\delta(t)$ appearing in Eq. (1) takes five different discrete values. It is common to take $\delta_i = -\pi, -\pi/2, 0, \pi/2, \pi$, $i = 1, 2, 3, 4, 5$. By substituting each of these five values into Eq. (1), one obtains five equations that allow us to write $\phi(x, y)$ in terms of the intensities $I_i(x, y)$ associated with each δ_i. That is, one obtains

$$\phi(x, y) = \tan^{-1}\left\{\frac{2[I_2(x, y) - I_4(x, y)]}{2I_3(x, y) - I_5(x, y) - I_1(x, y)}\right\}. \tag{3}$$

2.2 *Phase Unwrapping*

When phase shifting interferometry is used we must correct the discontinuities produced by the arc tangent function, see Eq. (3), which is only defined from $-\pi/2$ to $\pi/2$. The first correction is to extend the range from 0 to 2π. According to Schreiber and Bruning,[7] it is possible since the sign of the sine and cosine functions is well known independently of the tangent sign. The result is to produce the phase modulus 2π. We use Ghiglia's[4] method to unwrap the wavefront phase. This takes the wrapped phase differences with their adjacent neighbors and puts that difference in the modulus 2π. It is important to emphasize that the unwrapping procedure crucially depends on the selection of valid phase pixels (as was shown by Knoche et al.[8]) where the modulation equation is used to unwrap the phase.

2.3 *Geometrical Moments*

The geometrical moments[3] have been used to characterize the shape of an arbitrary object in computer vision systems. In the present work, following our previous research,[9] we use the geometrical moments to compute the boundary of an arbitrary interferogram. If the intensity $I(x, y)$ at the point (x, y) of a given interferogram is known then the geometrical moments associated with it are defined by

$$m_{pq} = \iint_{\tau} x^p y^q I(x, y) \mathrm{d}x\, \mathrm{d}y, \tag{4}$$

where $p, q = 0,1,2,3\ldots$, and τ is the surface region where the intensity function $I(x, y)$ is defined. The zero-order moment m_{00} represents the total intensity of any image and the first-order functions m_{10} and m_{01} give the intensity moments along the x and y axes of the image, respectively. The centroid (x_0, y_0) of the interferogram is defined by $x_0 = m_{10}/m_{00}$ and $y_0 = m_{01}/m_{00}$. This interferogram centroid was used as the origin of our reference system. The geometrical moments with respect to the centroid are called central moments and are defined by

$$\mu_{pq} = \iint_{\tau} (x - x_0)^p (y - y_0)^q \mathrm{d}x\, \mathrm{d}y. \tag{5}$$

Since we will record the interferogram aperture which is composed by a set of pixels in a CCD camera, then we need the geometrical moments and the central moments in the discrete case. Therefore, if $I(x, y)$ is the intensity of the interferogram at the pixel labeled with (x, y) then

$$m_{pq} = \sum_x \sum_y x^p y^q I(x, y),$$
$$\mu_{pq} = \sum_x \sum_y (x - x_0)^p (y - y_0)^q I(x, y), \tag{6}$$

where the sum is realized over the total pixels of the interferogram.

In this work, we consider optical systems with circular apertures. Therefore, we assume that the shape of the interferogram, in general, is an elliptical one characterized by the semi axis and the angle θ between the major semi axes and the x axes of the coordinate system with the origin at the centroid of the interferogram. A direct computation shows that[3]

$$a = 2\left\{\frac{(\mu_{20} + \mu_{02}) + [(\mu_{20} + \mu_{02})^2 + 4\mu_{11}^2]^{1/2}/2}{\mu_{00}}\right\}^{1/2},$$
$$b = 2\left\{\frac{(\mu_{20} + \mu_{02}) - [(\mu_{20} - \mu_{02})^2 + 4\mu_{11}^2]^{1/2}/2}{\mu_{00}}\right\}^{1/2}.$$
$$\theta = \frac{1}{2}\tan^{-1}\left(\frac{2\mu_{11}}{\mu_{20} - \mu_{02}}\right). \tag{7}$$

It is important to note that the first original contribution of the present work is to use the a, b, and θ parameters to find the valid and invalid phase pixels associated with a given interferogram, which is different from the method based in the modulation Eq. (2) reported in the literature.[10]

3 Detecting Valid Phase Pixels

When we are at the optical workshop testing an optical system, the phase of the fringe patterns digitized depends on the form of the boundary of the surface under test, which is commonly elliptical, although any other shape is possible as was shown by Castro- Ramos and Sasian.[11] However, the sensor of the CCD is rectangular giving us a rectangular digitized image, and for this reason, we have pixels with a valid phase in the ellipse and pixels with an invalid phase out of the ellipse. Remember that the pixels with a valid phase determine the fringe pattern. One of the most important methods to choose the valid phase pixels for fringe patterns is experimentally using the modulation equation introduced by Schreiber and Bruning and Creath,[7,10] which needs at least three interferograms. In this work, we use Hariharan's algorithm to compute

$$\gamma(x, y) = \frac{I''(x, y)}{I'(x, y)} = \frac{3\sqrt{4(I_2 - I_4)^2 + (I_1 + I_5 - 2I_3)^2}}{2(I_1 + I_2 + 2I_3 + I_4 + I_5)}, \tag{8}$$

and the Creath criteria[10] to determine the valid phase pixels. In accordance with Creath, a data modulation $\gamma(x, y)$ near one determines a valid phase pixel and a data modulation close to zero is an invalid phase pixel. Data points with a modulation below some threshold will have insufficient signal to noise ratio, so they are excluded from the analysis because the wavefront phase cannot be reliably calculated at those points. On the other hand, by using the geometrical

Table 1 Computed background equations and their correspondent modulation and wrapped phase equations.

Phase step size	Wrapped phase equation	Modulation equation	Background equation
$(0, \pi/2, \pi)$	$\tan\varphi = -\dfrac{-I_1 + 2I_2 - I_3}{I_1 - I_3}$	$\gamma(x,y) = \dfrac{\sqrt{(I_1 - I_3)^2 + (2I_2 - I_1 - I_3)^2}}{I_1 + I_3}$	$I_1 + I_3 = 255$
$(0, 2\pi/3, 4\pi/3)$	$\tan\varphi = -\sqrt{3}\dfrac{I_1 - I_3}{I_1 - 2I_2 + I_3}$	$\gamma(x,y) = \dfrac{\sqrt{(2.25)(I_1-I_3)^2+(0.75)(2I_2-I_1-I_3)^2}}{0.866(I_1+I_3+I_2)}$	$I_1 + I_2 + I_3 = 382$
$(0, \pi/2, \pi, 3\pi/2)$	$\tan\varphi = -\dfrac{I_2 - I_4}{I_1 - I_3}$	$\gamma(x,y) = \dfrac{2\sqrt{(I_4 - I_2)^2 + (I_1 - I_3)^2}}{I_1 + I_2 + I_3 + I_4}$	$I_1 + I_2 + I_3 + I_4 = 510$
$(0, 2\pi/3, 4\pi/3, 2\pi)$	$\tan\varphi = -\sqrt{3}\dfrac{I_2 - I_3}{I_1 - I_2 - I_3 + I_4}$	—	$I_1 + 2I_2 + 2I_3 + I_4 = 766$
$(0, \pi/4, \pi/2, 3\pi/4, \pi)$	$\tan\varphi = -\dfrac{I_1 + 4I_2 - 4I_4 + I_5}{I_1 + 2I_2 - 6I_3 + 2I_4 + I_5}$	—	$I_1 + I_5 = 255$
$(0, \pi/2, \pi, 3\pi/2, 2\pi)$	$\tan\varphi = -\dfrac{2(I_2 - I_4)}{2(I_3 - I_5 - I_1)}$	$\gamma(x,y) = \dfrac{3\sqrt{4(I_2 - I_4)^2 + (I_1 + I_5 - 2I_3)^2}}{2(I_1 + I_2 + 2I_3 + I_4 + I_5)}$	$2I_1 + 3I_2 + 4I_3 + 3I_4 + 2I_5 = 1785$
$(0, \pi/2, \pi, 4\pi/3, 2\pi, 5\pi/2)$	$\tan\varphi = -\dfrac{(I_1 + 3I_2 - 4I_4 - I_5 + I_6)}{(I_1 - I_2 - 4I_3 + 3I_5 + I_6)}$	—	$I_1 + 2I_3 + I_5 = 510$
$(0, \pi/3, 2\pi/3, \pi, 4\pi/3, 5\pi/3, 2\pi)$	$\tan\varphi = -\sqrt{3}\dfrac{I_2 + I_3 - I_5 - I_6}{I_1 + I_2 - I_3 + 2I_4 - I_5 + I_6 + I_7}$	—	$I_1 + I_2 + I_3 + 2I_4 + I_5 + I_6 + I_7 = 1020$

moments, we compute a, b, and θ which determine the region of the all valid phase pixels. As was pointed out above, this is the first original contribution of the present work. Observe that by using the equation of the modulation procedure we obtain one valid phase pixel at a time, while by using the geometrical moments, we are able to obtain all the valid phase pixels. This is the most important difference between the modulation equation and the geometrical moments procedures.

3.1 *Intensity-Based Selection of Valid Interferometric Data*

Assuming that the aperture is circular and making use of the intensity pattern Eq. (1), we find by simulating and analyzing five ideal fringe patterns with a phase shift of 90 deg between them that, for all the valid phase pixels the linear combination of gray levels intensities, gives

$$2I_1(x,y) + 3I_2(x,y) + 4I_3(x,y) + 3I_4(x,y) + 2I_5(x,y) = 1785, \tag{9}$$

and for the invalid ones equals zero. This is the second and the main result of the present work, which we call the background equation and it is analogous to the modulation equation. We want to point out that this equation will allow us to reconstruct the phase of the experimental fringe patterns by using Hariharan's PSI algorithm. In a similar manner, we found analogous results for several phase

shifting methods which we present in Table 1. In column 1 are the step sizes for the different PSI algorithms, in column 2 are their corresponding wrapped phase equations, in column 3 are the modulation equations reported in the literature (see Creath[10]), and in column 4 are the background equations that we compute for each PSI algorithm, where I_1, I_2, I_3, I_4, I_5, I_6 and I_7 are the intensities of the fringe patterns of each phase shift and $\phi(x, y)$ is the phase of the emerging measured wavefront.

3.2 *Threshold Equation*

To determine a valid phase pixel (x, y) of an experimental interferogram, we compute the value of the linear combination of the intensities appearing on the left-hand side of Eq. (9) at that pixel and compare this with the ideal constant, 1785. Then we choose a threshold value that goes from 1% to 100% of 1785. If the experimental value is lower than the threshold value, that pixel is invalid and if the experimental value is larger than the threshold one, then that pixel is a valid phase pixel.

The problem here was to select the best threshold value to make the comparison, because it depends on factors such as the irradiance of the source of illumination (i.e., laser or LED), the roughness, the reflectance of the mirror under test, the imaging lens of the CCD, and the background illumination. To solve this problem, we tested different mirrors varying the irradiance of the source, the coating of the mirror and its roughness. After that, the experimental fringe patterns were analyzed with different threshold values and we found that the unwrapping on borders crucially depends on the threshold selection. We made approximately 1000 unwrapping processes for several different mirrors, and only a hundred of them give good results. We plot the hundred experimental threshold constants versus the fringe intensities and we find a polynomial fitting to automatically select the value of the constant used for each series of interferograms given by

$$\text{Threshold}(\bar{I}) = -8.45471 + 0.38168\bar{I} - 0.0025\bar{I}^2 + 0.000010055\bar{I}^3, \quad (10)$$

where $\bar{I}$ is the average of the intensities of a fringe pattern, and the vertical axes give the desired threshold values used in the valid phase detection pixels of the fringe pattern.

As an example, in Fig. 1, we show the curve fitting of the third-order of the data and [Eq. (10)] is used to obtain an automatic threshold for any optical test that uses the Hariharan's algorithm. From our results, we find that to get a good unwrapping, in the majority of the tested optical systems, it is enough to choose a threshold of 15% of the ideal value.

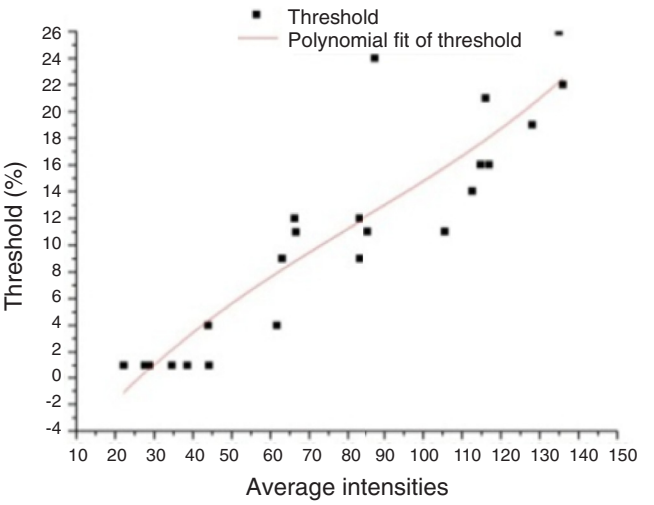

Fig. 1 Automatically computing the threshold value by polynomial fitting.

4 Experimental Setup and Software

Since our derived equations are valid for any kind of interferometer, in this section we apply them to obtain the wavefront phase by using the Ronchi and the Twyman–Green interferometers.

4.1 *Ronchi Test*

In Fig. 2, we show the setup of the Ronchi test. This arrangement consists of the mirror or lens under test, a liquid-crystal display (LCD) which allows us to instantaneously and automatically change the pitch of the Ronchi ruling, an interchangeable revolver of light-emitting diodes (LEDs) as the source of illumination (none of the LEDs use additional optical components, avoiding some additional aberrations during the test). We use several LEDs which cover a wavelength range from 450 to 950 nm, which increases the visibility of the polished or rough surfaces. We feed all LEDs employing a small power supply and a variable resistor to vary voltages in order to have the correct current and voltage to increase or reduce the intensity of the LED in use. The Ronchigrams were detected with a CCD camera of $640 \times 480 \times 1$ pixels and we wrote a software program in Visual C++ 2012 to compute the equations from Table 1 and to display the ruling on the LCD. Finally, another program was written to compute the background equations, the unwrapping phase, the transversal aberration, and the aberrated wavefront.

We carry out the experiment for a solid aluminum mirror with a diameter of 400 mm and a curvature radius of

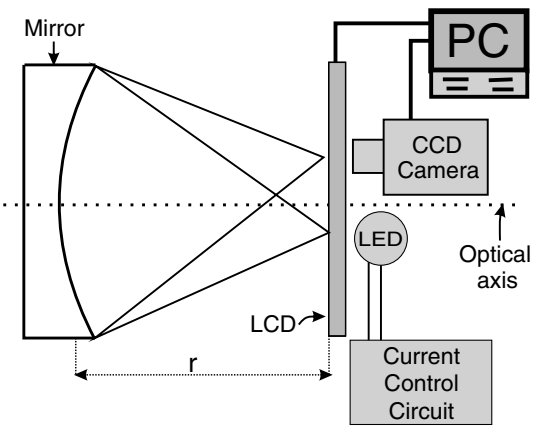

Fig. 2 Schematic drawing of the experimental setup to obtain lateral shear interferograms and the wavefront phase with the proposed background equations.

150 mm with a hole in its center. In Fig. 3, we show some fringe patterns obtained for this mirror. Observe that all the figures have a good contrast because our device allows us to vary the wavelength and the intensity of the LED used as the illumination source. Figures 3(a) to 3(e) are five vertical ronchigrams obtained by doing a horizontal phase shift of $\pi/2$. Figures 3(f) to 3(j) are five horizontal ronchigrams obtained by doing a vertical phase shift of $\pi/2$. Figures 3(k) and 3(n) show the modulation and background equations with a threshold of 5. We can see that the background equation includes fewer pixels outside the aperture than the modulation equation. Figures 3(l) and 3(o) show the modulation and background equations with a threshold of 25. The threshold is increased, but the valid phase pixels detection does not improve in the modulation equation when it is compared with the background equation. Figures 3(m) and 3(p) show the modulation and background equations with a threshold of 50. Pixel detection outside the aperture does not improve for the modulation equation and many pixels are lost. However, the background equation gives more details and we can see the central hole of the mirror under test. In Fig. 3(q), we present the horizontal transversal aberration, in Fig. 3(r) we show the vertical transversal aberration and finally, in Fig. 3(s), we present the wavefront plot. From Figs. 3(n) to 3(p), we conclude that our method is robust because we do not need to turn the light off to get valid phase pixels.

4.2 *Validation of Intensity-Based Selection of Valid Phase Data*

Now we show that our background equation provides good qualitative results in obtaining the wavefront. To this end, we compare our results with those obtained by using the

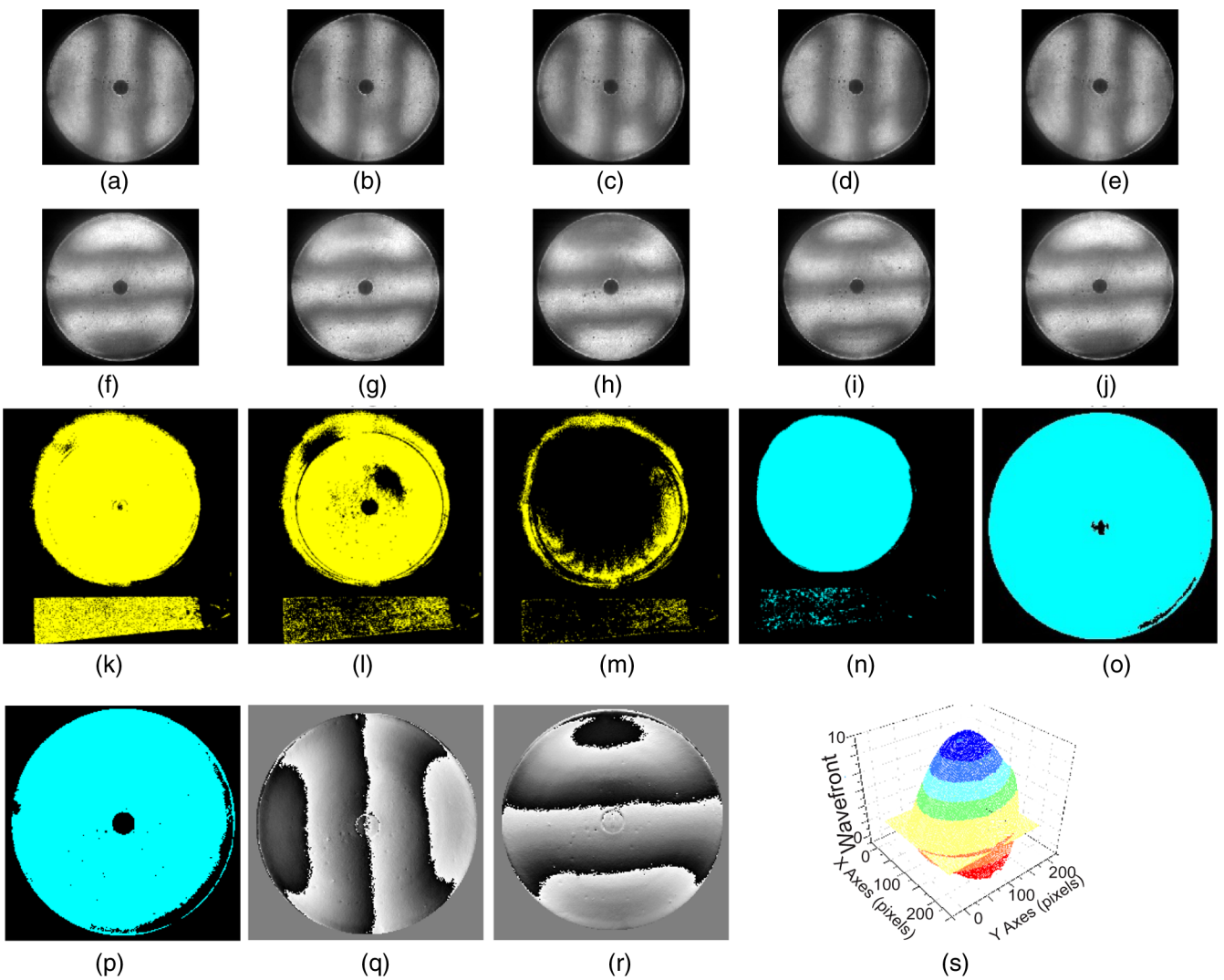

Fig. 3 Analysis of lateral shear fringe patterns obtained experimentally. Figures (a) to (e) with a horizontal phase shift of $\pi/2$. Figures (f) to (j) with a vertical phase shift of $\pi/2$. Figures (k) to (m) masks obtained with the modulation equation with a threshold of 5, 25, and 50. Figures (n) to (p) masks obtained with the background equation with a threshold of 5, 25, and 50, respectively, (q) horizontal transversal aberration, (r) vertical transversal aberration, and (s) the wavefront.

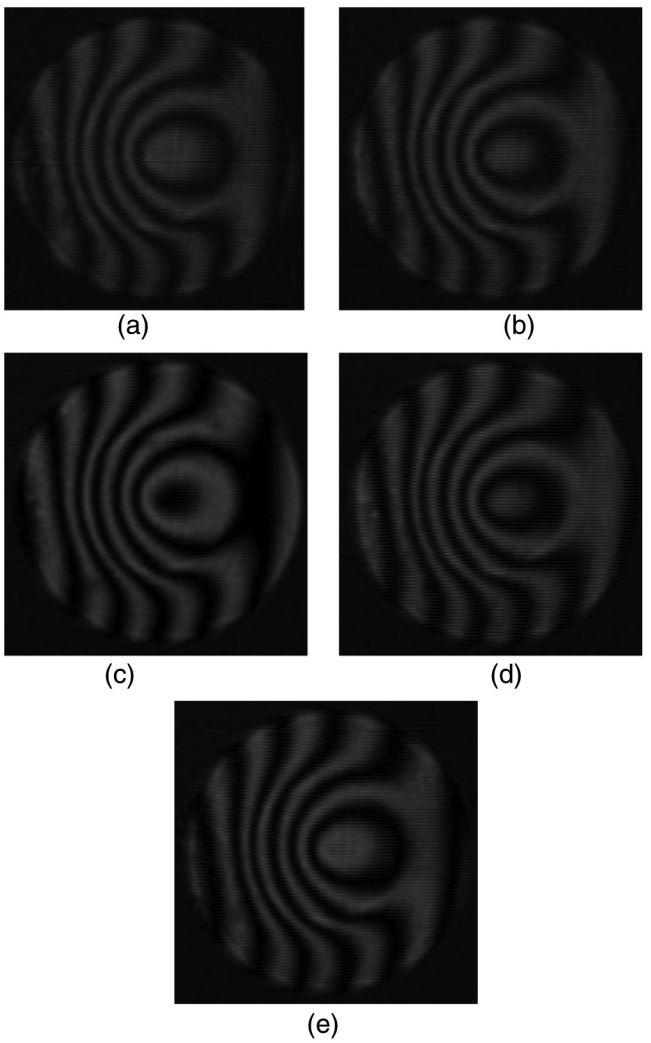

Fig. 4 Interferograms obtained with the Twyman–Green interferometer and analyzed with Durango® software with (a) 0 deg of phase shift, (b) 90 deg of phase shift, (c) 180 deg of phase shift, (d) 270 deg of phase shift, and (e) 360 deg of phase shift.

Twyman–Green interferometer, which directly provides the wavefront.

We start by fixing our own arrangement of the Twyman–Green interferometer to get five $\pi/2$ phase shift interferograms of an uncoated hyperbolic polished glass mirror, presented in Fig. 4. From this information and the implementation of a program in visual C++ 2012, which takes into account Eqs. (8) and (9) and the geometrical moments, we determine the best circle associated with the interferograms, see Fig. 5. Finally, by using Eq. (3) and the Giglias's method we get the wavefront, see Fig. 7(a).

On the other hand, by using a commercial Twyman–Green interferometer and the Durango® software,[5] we obtain the valid phase pixels presented in Fig. 5. More specifically, we present the valid phase pixels using: 5(a) the modulation equation of Creath, 5(b) the modulation equation computed by Durango software and 5(c) our background equation, which corresponds to the circle mask automatically calculated with the geometrical moments.[3,9] It is important to emphasize that using the background equation to compute the valid phase pixels has some additional advantages because we do not need to choose the boundary by hand and we do not need to turn the light off. In Fig. 6(a), we show the wrapped phase given by Durango® calculated with the circular aperture whole image, 6(b) shows the wrapped phase computed by Durango® calculated with the circular aperture that we select manually, and in Fig. 6(c), we show the wrapped phase given by our software calculated with the circular aperture which was automatically calculated using the geometrical moments and the background equation. In Fig. 7(a), we show the wavefront obtained after unwrapping the phase with Giglia's method, and in 7(b) we show the wavefront obtained with Durango. As we can see, both results are similar, and with these results, we determine that our background equations, which were programmed in software, works correctly.

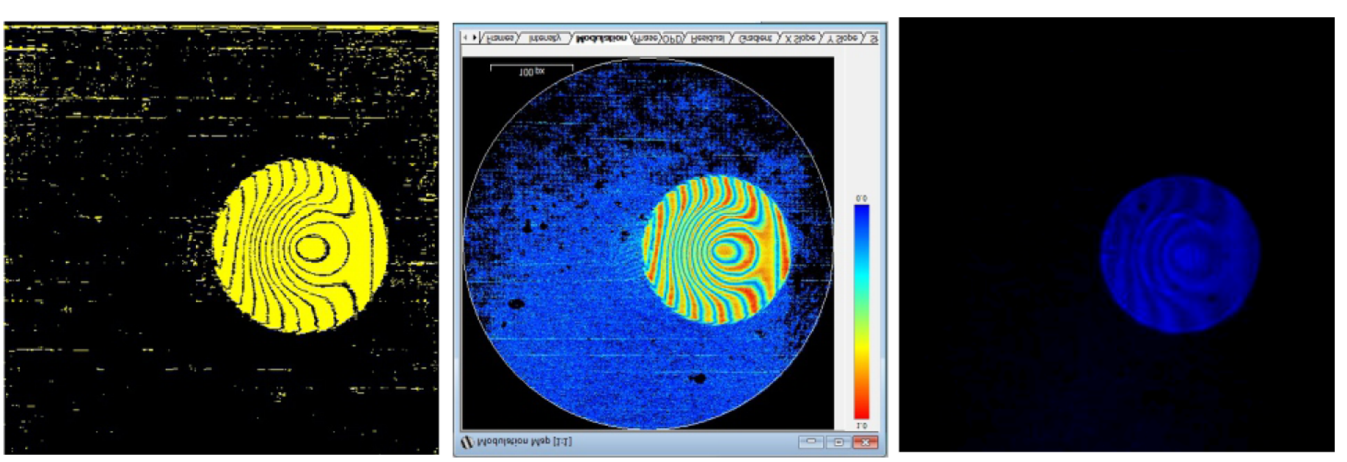

Fig. 5 The valid phase pixels using (a) the modulation equation of Creath, (b) the modulation equation computed by Durango software, and (c) our background equation.

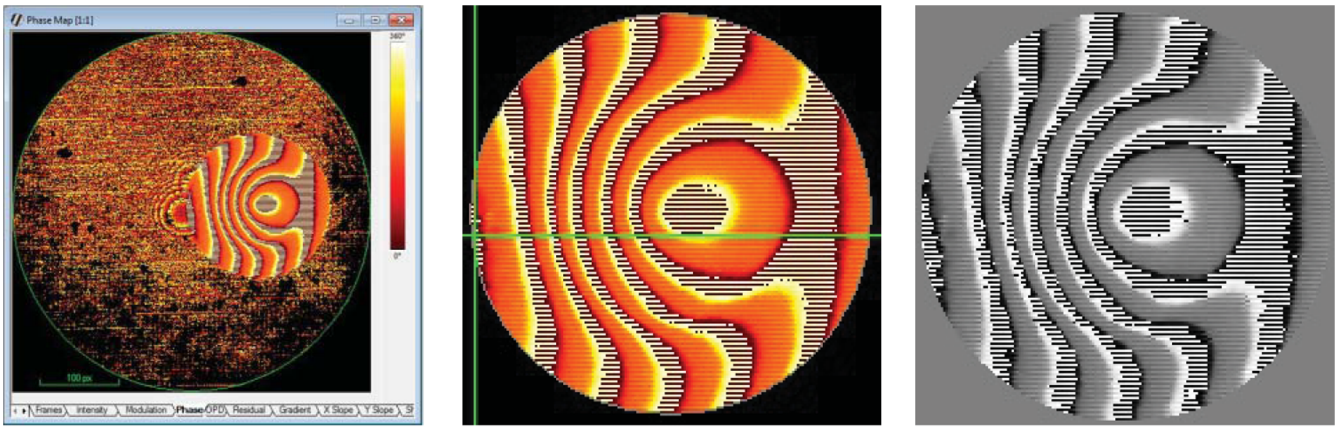

Fig. 6 (a) The wrapped phase by Durango for the whole image, (b) the wrapped phase by Durango for a chosen circular aperture, and (c) the wrapped phase with our software. From (b) and (c), it is clear that they are similar.

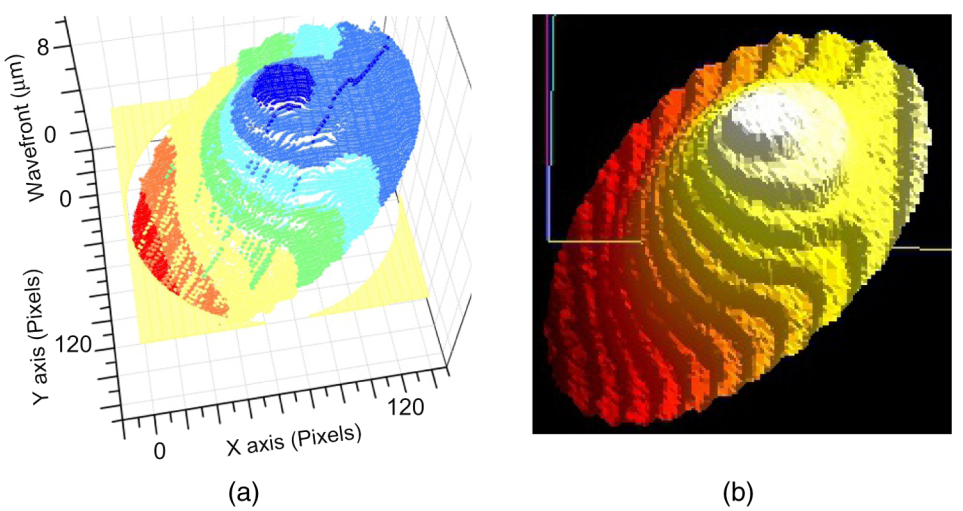

Fig. 7 (a) The wavefront obtained with our proposed equation and (b) the wavefront obtained with Durango software.

5 Conclusion

We proposed a method to detect valid phase pixels, which was proven with the Twyman–Green and the Ronchi interferometers using the phase shifting interferometric technique. From the qualitative results presented in Figs. 3(k) to 3(p), 5, and 6, we conclude that our method is better than the modulation equation because there are fewer pixels outside the interferogram aperture. Furthermore, we found the corresponding background equations for different PSI algorithms, which also allows us to detect the valid phase pixels, presented in fourth column of Table 1. We programed our method and the results of our software were compared with the commercial software Durango; similar results were achieved with both methods. Furthermore, with our method we have the advantage that we do not need to manually choose the boundary. It is automatically computed with the geometrical moments in spite of the fact that we do not turn off the light to digitize the interferograms. Every commercial interferometry fringe analysis program is good enough to provide the wavefront aberration, but the method proposed here gives another alternative and may be of interest for several fields of interferometric metrology.

Acknowledgments

The authors acknowledge the comments received from two referees to improve the presentation of this work. Furthermore, we thank F. Salomon-Granados, E. Percino-Zacarias, for their help in the use of Durango and also thank G. Gordiano-Alvarado and L. Sastre-Juarez for their help in the electronics. GSO acknowledges the financially support received from SNI (México) and VIEP-BUAP.

References

1. M. Born and E. Wolf, *Principles of Optics*, 7th ed., Cambridge University Press, United Kingdom (1999).
2. D. Malacara, *Optical Shop Testing*, 3rd ed., John Wiley & Sons Inc., New Jersey (2007).

3. R. Mukundan and K. R. Ramakrishnan, *Moment Functions in Image Analysis Theory and Aplications*, Wok Scientific Publishing CO. Pte Ltd., Singapore, pp. 9–37, 127–128 (1998).
4. D. C. Ghiglia and L. A. Romero, "Robust two-dimensional weighted and unweighted phase unwrapping that uses fast transforms and iterative methods," *J. Opt. Soc. Am. A* **11**(1), 107–117 (1994).
5. Diffraction International©, "Durango, Interferometry Software," Updated 17 October 2014, http://www.diffraction.com/durango_software.php (9 December 2014).
6. K. P. Hariharan, B. F. Oreb, and T. Eiju, "Digital phase shifting interferometry: a simple error-compensating phase calculation algorithm," *Appl. Opt.* **26**(13), 2504 (1987).
7. H. Schreiber and J. H. Bruning, Chapter 14 in *Optical Shop Testing*, D. Malacara, Ed., 3rd ed., p. 547, John Wiley, Hoboken, New Jersey (2007).
8. S. Knoche et al., "Modulation analysis in spatial phase shifting electronic speckle pattern interferometry and application for automated data selection on biological specimens," *Opt. Commun.* **270**, 68–78 (2007).
9. J. Sánchez-Paredes et al., "1λ Ronchi tester to obtain the wave front aberration in converging optical systems using phase shifting interferometry," *Opt. Pura Apl.* **45**(4), 461–473 (2012).
10. K. Creath, "Phase measurement interferometry techniques," in *Progress in Optics*, Vol. XXVI, E. Wolf, Ed., pp. 349–393, Elsevier Science Publishers, Amsterdam (1998).
11. J. Castro-Ramos and J. Sasian, "Automatic phase shifting Ronchi tester with a square Ronchi ruling," *Proc. SPIE* **5532**, 199–210 (2004).

Jaime Sánchez-Paredes received his BSc degree in electronics at the Instituto Tecnológico de Apizaco in 2003 and his MSc and PhD degrees in optics from the Instituto Nacional de Astrofísica Óptica y Electrónica (INAOE), Mexico, in 2007 and 2013, respectively. His main research interests include optical testing, phase shifting interferometry, and digital image processing.

Gilberto Silva-Ortigoza received his PhD Degree in physics in 1995 at CINVESTAV-IPN, Mexico. His lines of research are general relativity and geometrical optics.

Jorge Castro-Ramos received his PhD degree in optics in 2000 at INAOE, where he has been working as researcher in optics since 2004. His principal interest is in optical shop testing and biophotonics.